Uncertainties in Performance Based Design Methodologies for Seismic Microzonation of Ground Motion and Site Effects: State of Development and Applications for Italy

Salvatore Grasso [1] and Maria Stella Vanessa Sammito [1]

[1] Department of Civil Engineering and Architecture, University of Catania (Italy)
sgrasso@dica.unict.it

Abstract. Performance-Based Design (PBD) is a more rational and general design approach, particularly for seismic regions, in which the design criteria are expressed in terms of achieving stated performance objectives. In this approach it is relevant the performance required to structures and to geotechnical works subjected to stated levels of seismic hazard, as well as the geotechnical constitutive model used to predict the performance. The parameters of the constitutive models are related in turn to soil properties. Earthquake hazard zonation in urban areas is the first and most important step towards a seismic risk analysis in densely populated Regions. The Seismic Microzonation is nowadays a worldwide accepted tool for the mitigation of seismic risk. It is a complex process involving different disciplines ranging from Geology and Applied Seismology to Geotechnical and Structural Engineering. The aim achieved in seismic hazard microzonation studies throughout the last 20 years performed at the presented typical case histories in Italy was to quantify the spatial variability of the site response on some typical historical scenario earthquakes that would be expected in the area. In order to quantify the expected ground motion, the manner in which the seismic signal is propagating through the subsurface was defined.

Propagation was particularly affected by the local geology and by the geotechnical dynamic ground conditions. Large amplification of the seismic signals generally occurs in areas where layers of low seismic shear wave velocity overlie material with high seismic wave velocity, i.e. where soft sediments cover bedrock or more stiff soils. Therefore, essential key issue here is to obtain a good understanding of the local subsurface conditions. The study builds on the recent experience of seismic microzonation studies in Sicily (Italy), after the effects of the 2018 seismic sequence. Examples of ground response analysis are presented by using some 1-D and 2-D codes, including methodologies taking into account soil uncertainties for site characterisation.

Keywords: Seismic Microzonation Studies, Spectrum Compatibility, 1D and 2D Numerical Analyses

1 Introduction

This paper describes the Performance Based Design (PBD) methodology for the Seismic Microzonation (SM) of ground motion and site effects. One of the most important aspects is the definition of the input motions at the seismic outcropping bedrock based on the reference response spectra provided by the Italian seismic code[1] from probabilistic seismic hazard analysis. The suites of spectrum-compatible accelerograms can be used for 1D or 2D ground response analyses.

Another important aspect is the knowledge of the geological, geotechnical and geophysical characteristics of the areas under consideration in order to define the subsoil models [2]. On the basis of this methodology, it is possible to obtain a detailed delineation of the spatial variability in seismic responses, which can be used for the seismic microzonation mapping [2-3].

Although probabilistic hazard analyses could be helpful in selecting sets of accelerograms, a deterministic evaluation is preferred in areas where large and rare earthquakes are observed [4-7]. The use of advanced methods capable of generating synthetic seismograms can give a valuable insight into the evaluation of a seismic ground motion scenario [4].

After the intense Etna seismic activity that began on 23 December 2018 and characterized by about seventy events with a magnitude M > 2.5, seismic microzonation studies were performed in Sicily (Italy) with the aim of supporting the structural design of buildings and the urban planning.

The studies have been carried out in several municipalities located in the region of Sicily (Riposto, Acireale, Piedimonte Etneo, Zafferana Etnea, Milo, Termini Imerese, Cefalù, Finale di Pollina, Trabia, Campofelice di Roccella, Alì Terme, Salaparuta, Balestrate and Caronia).

2 Historical earthquakes in Sicily

Sicily is one of the Italian regions with high seismic risk. It was shaken in the past by large destructive events (1169, 1542, 1693, 1818, 1848, and 1990) [8-9]. A repetition of events with similar characteristics would provide the additional risk of a damaging tsunami, as well as, liquefaction phenomena around the coastal areas of Sicily [10-11].

The Val di Noto earthquake of January 11, 1693, struck a vast territory of southeastern Sicily and caused the partial, and in many cases total, destruction of 57 cities and 60,000 casualties [12–13]. The Etna earthquake that took place on February 20, 1818, was a moderate earthquake, but its effects were noticed over a vast area [14-16]. The largest damage was observed in Augusta, where almost two-thirds of the buildings collapsed [9, 17]. On December 1908, a devastating earthquake occurred along the Strait of Messina between eastern tip of Sicily and the western tip of Calabria in the south of Italy. The Southern Calabria-Messina earthquake (Intensity MSC XI, Mw 7.24) was the strongest seismic event of the 20th century in Italy with the most ruinous in term of casualties (at least 80,000) [18].

More recently, the 26 December, 2018, earthquake (Mw 4.9) occurred at shallow depth (<1 km) on the eastern flank of Mount Etna. It was the most energetic event that hit the volcanic area during the last 70 years [19]. Figure 1 shows the intensity maps for the 1693, 1818, 1908 and 2018 earthquakes.

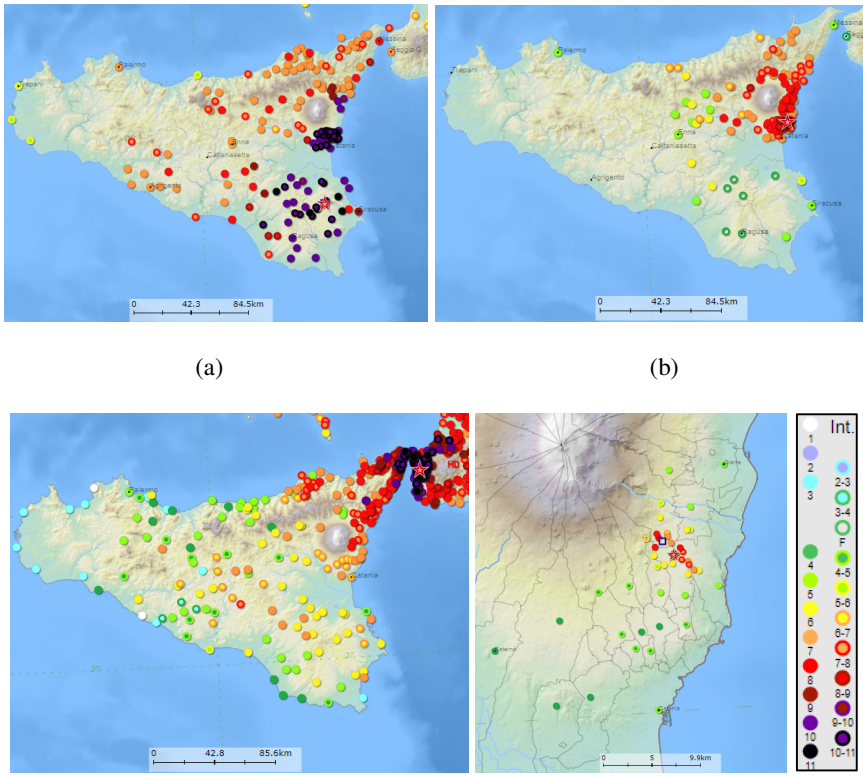

(a) (b)

(c) (d)

Fig. 1. Intensity maps: a) earthquake of 11 January, 1693; b) earthquake of 20 February, 1818; c) earthquake of 28 December, 1908; d) earthquake of 26 December, 2018 [20-21]

3 Geology and site characterization programme

Sicily, located on the Pelagian promontory of the African plate, is formed by the Iblean foreland, the Gela foredeep, the thick Sicilian orogen and the thick-skinned Calabrian-Peloritani wedge. The topography and geomorphology of Sicily is the result of constructive and destructive forces following the collision between the African and European plates [22]. The geological map of Sicily is reported in Figure 2.

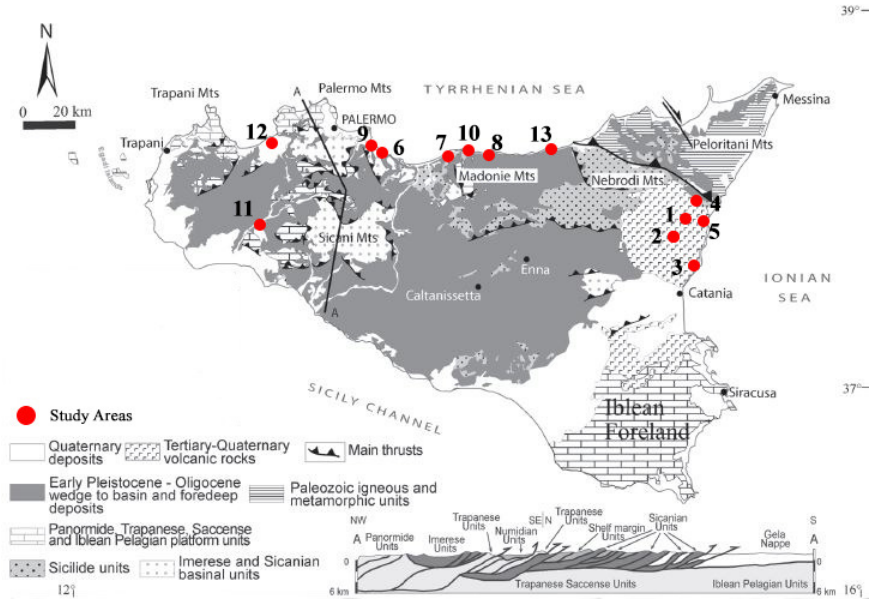

Fig. 2. Geological map of Sicily (data compiled from various Authors [23-24] and simplified from [22]; modified) and location of the study areas.

The geotechnical and geophysical characterization of the study areas, whose locations are shown in the Figure 2, has required an accurate field investigation that reached the depth of 30 m. Moreover, laboratory tests have been also performed on undisturbed samples. Laboratory and in situ investigations include the following tests: Boreholes, Down Hole Tests (DH), Multichannel Array Surface Wave Tests (MASW), Seismic Tomographies, Horizontal to Vertical Spectral Ratio Tests (HVSR) and Direct Shear Tests (DST).

Shear wave velocity, V_s, plays a fundamental role in Seismic Microzonation Studies. Therefore, in order to summarize V_s profiles against depth obtained by geophysical tests, the equivalent shear wave velocity ($V_{s,eq}$) has been calculated for each test sites according to the Italian seismic code [1]. $V_{s,eq}$ values and the corresponding soil types [1] are reported in Table 1.

Table 1. Equivalent shear wave velocities and soil types obtained from geophysical tests according to the NTC 2018[1]

	Test sites	$V_{s,eq}$ [m/s]	Soil Types
1	Milo	384	B
2	Zafferana Etnea	449	B
3	Acireale	343	C
4	Piedimonte Etneo	504	B
5	Riposto	458	B

6	Termini Imerese	466	B
7	Campofelice di Roccella	389	B
8	Finale di Pollina	397	B
9	Trabia	486	B
10	Cefalù	365	B
11	Salaparuta	291	C
12	Balestrate	261	C
13	Caronia	388	B

4 Selection of sets of input ground motions

The Italian seismic code [1] adopts the performance-based seismic design for the calculation of seismic actions on structures from probabilistic seismic hazard analysis (PSHA). The structural performance is verified against ground motions (GM) that have predetermined exceedance return periods at the site of interest. The corresponding GM is represented by the uniform hazard spectrum (UHS) [25].
The Italian seismic code [1] is based on the work of the National Institute of Geophysics and Volcanology (INGV) [26]. The INGV (http://esse1-gis.mi.ingv.it) evaluated the probabilistic seismic hazard for each node of a regular grid that covers the Italian territory. This resulted in hazard curves that are lumped in nine probabilities of exceedance in 50 years (2%, 5%, 10%, 22%, 30%; 39%, 50%, 63% and 81%) [26-27]. The interactive seismic hazard map of Sicily (Figure 3) has been obtained from http://esse1-gis.mi.ingv.it considering the 10% probability of exceedance in 50 years (return period of 475 years) that is the case of design for life-safety structural performance (SLV) [1].
The disaggregation data have been also derived (Figure 4) considering the latitudine and longitudine of each test site. Disaggregation, expressed in terms of magnitude (M), source to site distance (R) and standard deviations (ε), identifies the values of some earthquake characteristics providing the largest contributions to the hazard in terms of exceeding a specified spectral ordinate threshold [26].
The software REXEL v. 3.5 (http://www.reluis.it) [27] allows to search for suites of waveforms, from the European Strong-motion Database, compatible to the reference spectrum in a defined range of periods according to the Italian seismic code [1]. A combination of seven accelerograms has selected for each test site in a way that their average is in an interval between 10% (lower threshold) and 30% (upper threshold) of the reference spectrum. The range of periods is equal to 0.1-1.1 s that is representative of the vibration periods of the structures target. The Magnitude-Distance Criterion has been used considering the disaggregation data derived from http://esse1-gis.mi.ingv.it website. The accelerograms have not been scaled.

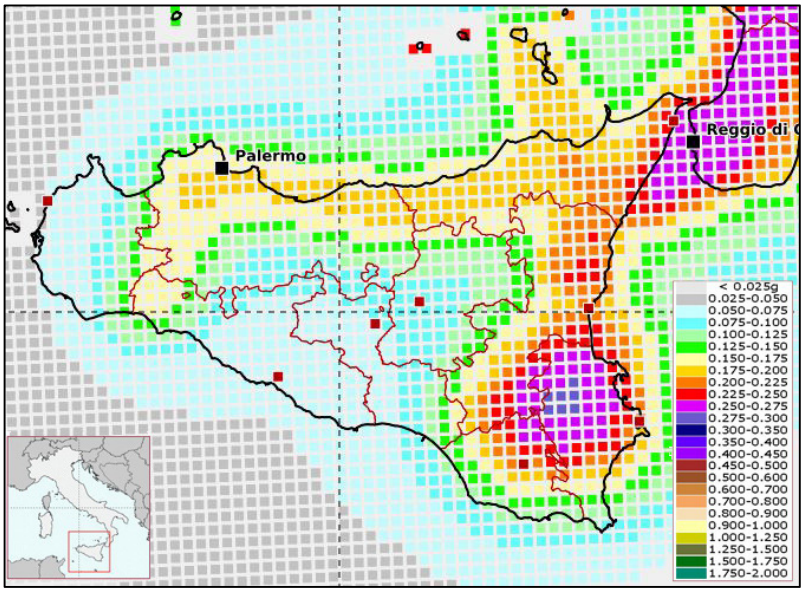

Fig. 3. Interactive seismic hazard map of Sicily considering the 10% probability of exceedance in 50 years (from http://esse1-gis.mi.ingv.it; modified)

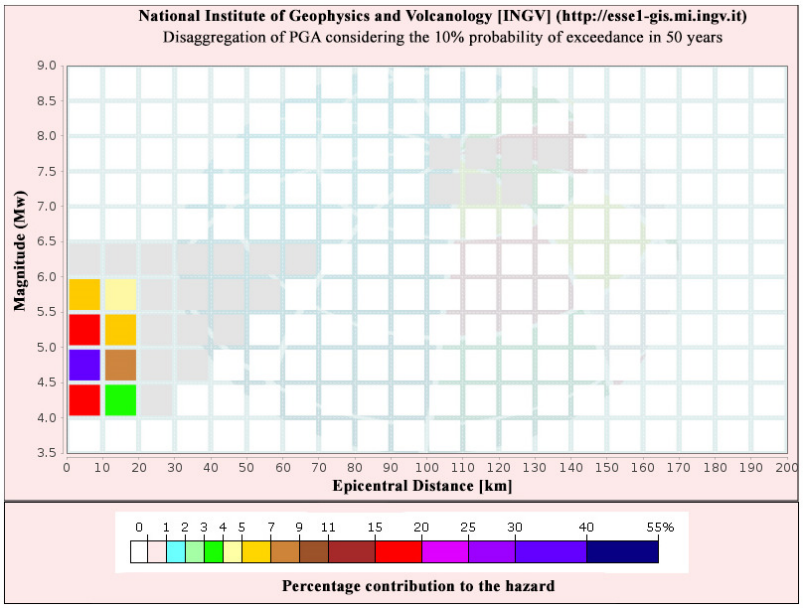

Fig. 4. Disaggregation data for Campofelice di Roccella (lat. 38.005; lon. 13.905) (from http://esse1-gis.mi.ingv.it; modified)

Table 2 and Figure 5 report the suites of waveforms compatible to the reference spectra (Soil Class A) [1] for Campofelice di Roccella (lat. 38.005; lon. 13.905), as an example, considering the 10% probability of exceedance in 50 years, the minimum event magnitude M_{min}=4.0, the maximum event magnitude M_{max}=6.5; the minimum epicentral distance R_{min}[km]=0 and maximum epicentral distance R_{max}[km]=20.

Table 2. Combination of waveforms obtained from REXEL v. 3.5. for Campofelice di Roccella (lat. 38.005; lon. 13.905)

Waveform ID	Earthquake ID	Station ID	Earthquake Name	Date	Mw	R[km]
982	72	ST309	Friuli (aftershock)	16/09/1977	5.4	9
4675	1635	ST2487	South Iceland	17/06/2000	6.5	13
242	115	ST225	Valnerina	19/09/1979	5.8	5
5079	1464	ST2552	Mt. Hengill Area	04/06/1998	5.4	6
6115	2029	ST1320	Kozani	13/05/1995	6.5	17
2025	710	ST1357	Kremidia (aftershock)	25/10/1984	5	16
4674	1635	ST2486	South Iceland	17/06/2000	6.5	5
mean					5.9	10.1

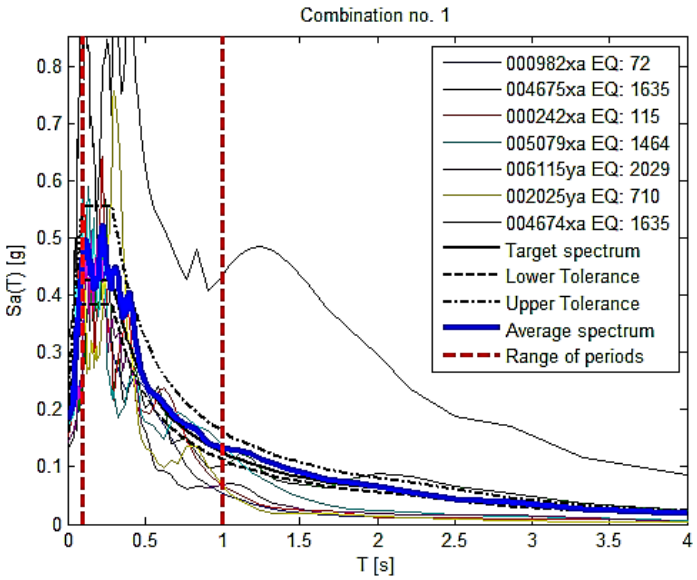

Fig. 5. Combination of waveforms obtained from REXEL v. 3.5. for Campofelice di Roccella (lat. 38.005; lon. 13.905)

A deterministic evaluation has been preferred for a slope located in Caronia test site, also because it can better account the complex heterogeneity of the area. Seven different inputs have been used, consisting of six synthetic seismograms related to the

Messina and Reggio Calabria 1908 earthquake (Bottari et al. [29]; Tortorici et al. [30]; Amoruso et al. [31]; DISS Aspromonte Est; DISS Gioia Tauro; DISS Messina Strait) and one related to the 1693 Catania scenario earthquake [32–33]. The seismograms have been scaled to the PGA of 0.176 g provided by the NTC2018[1].

5 Definition of the subsoil models

The definition of the subsoil model requires the knowledge of the depth of bedrock and the characterization of the soil layers in terms of geometry, geophysical and geotechnical properties. Moreover, laws of shear modulus and damping ratio against strain have to be considered in order to take into account the soil non linearity. For the estimation of the local site responses, 1D and 2D numerical analyses have been carried out.

5.1 1D Numerical Analyses

Local site response analyses have been performed using 1-D linear equivalent code STRATA [34] assuming the geometric and geological models as 1-D physical models. The equivalent linear analysis consists in the execution of a sequence of complete linear analysis with subsequent update of the parameters of stiffness and damping until the satisfaction of a predetermined convergence criterion [35].

The V_S profiles used for soil response analyses have been derived from geophysical tests reported in Paragraph 3. The value of the other parameters have been taken from the geotechnical characterization obtained through in situ and laboratory tests. In order to consider the degradation of the shear modulus and the increase of the damping ratio with the shear strain levels, Equations (1) and (2) suggested by Yokota et al. [36], calibrated to the soil under consideration, have been used.

$$\frac{G(\gamma)}{G_o} = \frac{1}{1+\alpha\gamma(\%)^{\beta}} \tag{1}$$

where: $G(\gamma)$ = strain dependent shear modulus; γ = shear strain; α, β = soil constant.

$$D(\gamma)(\%) = \eta \cdot \exp\left[-\lambda \cdot \frac{G(\gamma)}{G_o}\right] \tag{2}$$

where: $D(\gamma)$ = strain dependent damping; γ = shear strain; η, λ = soil constant. Table 1 shows the obtained soil constants. The G-γ and D-γ curves are reported in Table 3.

Table 3. G- γ and D- γ curves used for site response analyses

Curves	α	β	η	λ
1	7.5	0.897	90	4.5
2	6.9	1	23	2.21
3	16	1.2	33	2.4

4	linear	linear	linear	linear
5	9	0.815	80	4
6	20	0.87	19	2.3
7	22	1.05	10	1.05

5.2 2D Numerical Analyses

To evaluate topographic and stratigraphic effects, 2-D equivalent-linear site response analyses have been also performed by the QUAKE/W [37] code based on a finite element formulation with a direct integration scheme in the time domain.

Local seismic amplification has been studied for a slope located in Caronia area in order to determine the topographical contribution on the ground acceleration.

Figure 6 shows the cross-section used for the finite element analyses. Three-surface points have been monitored: (1) the first behind the crest of the slope, (2) the second at the crest of the slope, (3) the third at a point downstream sufficiently far from the foot of the slope.

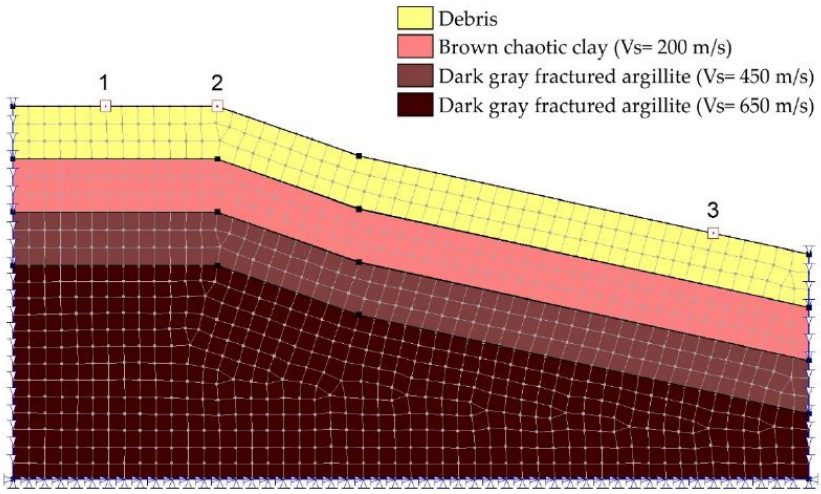

Fig. 6. Finite element model used for 2-D equivalent-linear site response analyses in Caronia area

6 Main Results

In the following, the main results obtained by numerical analyses have been summarized for all of the test sites considering the mean of the values calculated using the sets of seven input ground motions. Moreover, two case studies have been chosen (Campofelice di Rocella and Caronia) to outline specific results.

The soil dynamic response has been investigated in terms of accelerations. The values of the mean surface maximum accelerations and mean soil amplification factors, R, for all of the test sites, are reported in Table 4. The stratigraphic amplification values, S_s, provided by Italian technical code [1], are also presented for each test sites.

Table 4. Mean surface maximum accelerations and the mean soil amplification factors.

	Test sites	$PGA_{m,i}$	$PGA_{m,o}$	$R=PGA_{m,o}/PGA_{m,i}$	Ss
1	Milo	0.282 g	0.410 g	1.453	1.164
2	Zafferana Etnea	0.282 g	0.337 g	1.195	1.164
3	Acireale	0.282 g	0.439 g	1.554	1.345
4	Piedimonte Etneo	0.282 g	0.480 g	1.701	1.164
5	Riposto	0.282 g	0.476 g	1.688	1.164
6	Termini Imerese	0.173 g	0.262 g	1.513	1.200
7	Campofelice di Roccella	0.184 g	0.269 g	1.460	1.200
8	Finale di Pollina	0.184 g	0.345 g	1.877	1.200
9	Trabia	0.173 g	0.270 g	1.561	1.200
10	Cefalù	0.188 g	0.322 g	1.710	1.200
11	Salaparuta	0.178 g	0.310 g	1.743	1.463
12	Balestrate	0.148 g	0.274 g	1.849	1.500

In Figure 7, results are presented for Campofelice di Roccella in terms of mean response spectrum at the surface, obtained by setting a structural damping of 5%. The elastic response spectrum provided by the Italian seismic code [1] is also shown. Moreover, according to the guidelines for Seismic Microzonation studies [38], FA factors have been determined for each test sites from the input and output spectra (Table 5) according to the following procedure:

1. Calculation of the period corresponding to the maximum spectral acceleration of the input spectrum ($S_{e,max,i}$): TA_i;
2. Calculation of the period corresponding to the maximum spectral acceleration of the output spectrum ($S_{e,max,o}$): TA_o;
3. Calculation of the mean value of the input spectrum in $0.5TA_i$ and $1.5TA_i$: $SA_{m,i}$:

$$SA_{m,i} = \frac{1}{TA_i}\int_{0.5TA_i}^{1.5TA_i} SA_i(T)dt \quad (3)$$

4. Calculation of the mean value of the output spectrum in $0.5TA_o$ and $1.5TA_o$: $SA_{m,o}$:

$$SA_{m,o} = \frac{1}{TA_o}\int_{0.5TA_0}^{1.5TA_0} SA_o(T)dt \quad (4)$$

where $SA_i(T)$ is the input spectrum and $SA_o(T)$ is the output spectrum;

5. Calculation of $FA= SA_{m,o}/ SA_{m,i}$

Figure 8 shows the amplification functions, A(f), for Campofelice di Roccella evaluated as the ratio between the Fourier spectra at the surface level and the Fourier spec-

tra of the input motions applied at the base of the model. The main resulting frequencies f(I) and f(II) obtained by numerical analyses for each test site are reported in Table 6.

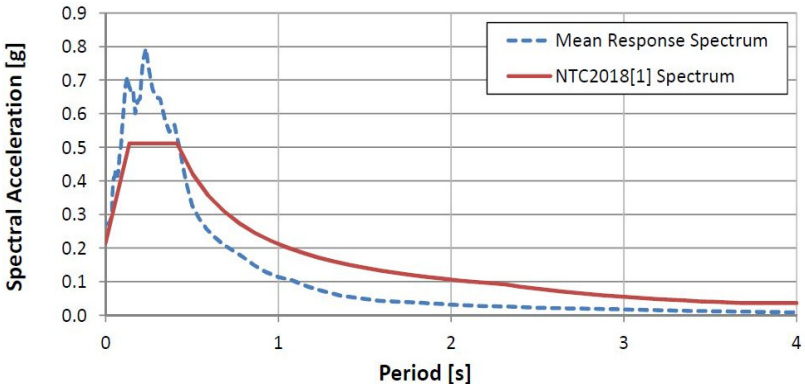

Fig. 7. Comparison between the mean elastic response spectrum obtained by numerical analyses and the same provided by NTC 2018[1]

Table 5. Values of FA factors

Test sites	$Se_{max,i}$[g]	TA_i[s]	$Se_{max,o}$[g]	TA_o[s]	$SA_{m,i}$	$SA_{m,o}$	FA
1	0.73	0.20	0.99	0.40	0.62	0.87	1.41
2	0.73	0.20	0.91	0.43	0.62	0.72	1.16
3	0.73	0.20	1.07	0.43	0.62	0.87	1.41
4	0.73	0.20	1.52	0.20	0.62	1.09	1.75
5	0.73	0.20	1.21	0.20	0.62	1.04	1.69
6	0.52	0.22	0.81	0.22	0.45	0.69	1.52
7	0.51	0.22	0.79	0.23	0.46	0.68	1.46
8	0.52	0.24	1.34	0.22	0.46	0.98	2.13
9	0.52	0.22	0.72	0.12	0.44	0.64	1.44
10	0.47	0.19	0.83	0.06	0.39	0.53	1.36
11	0.50	0.12	0.86	0.15	0.40	0.72	1.79
12	0.36	0.15	0.76	0.20	0.33	0.63	1.88

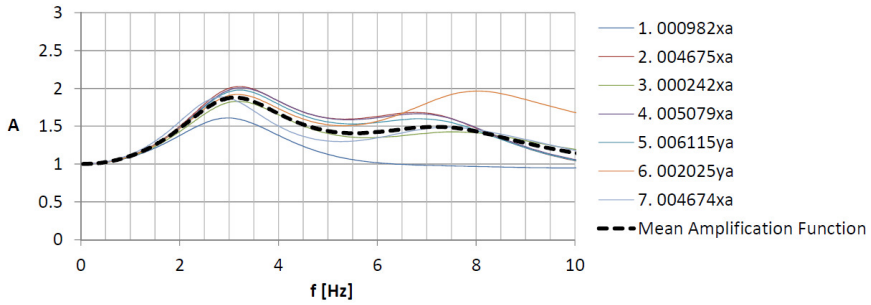

Fig. 8. Amplification functions obtained by numerical modelling for Campofelice di Roccella

Table 6. Main resulting frequencies f(I) and f(II) obtained by numerical analyses

	Test sites	f(I)[Hz]	f(II)[Hz]
1	Milo	2.59	8.34
2	Zafferana Etnea	2.89	12.65
3	Acireale	1.99	6.19
4	Piedimonte Etneo	6.30	15.35
5	Riposto	4.02	11.06
6	Termini Imerese	5.26	11.57
7	Campofelice di Roccella	3.10	7.08
8	Finale di Pollina	4.81	15.81
9	Trabia	6.10	13.62
10	Cefalù	2.99	6.77
11	Salaparuta	2.29	5.66
12	Balestrate	2.28	5.58

Topographic seismic effects have been evaluated for the slope located in Caronia area. Three measures of amplifications have been computed [39]: the topographic amplification, A_t; the site amplification, A_a; the apparent amplification, A_a. The following equations have been used:

$$A_t = \frac{a_{max} - a_{ffc}}{a_{ffc}} \quad (5)$$

$$A_s = \frac{a_{ffc} - a_{fft}}{a_{fft}} \quad (6)$$

$$A_a = \frac{a_{max} - a_{fft}}{a_{fft}} \quad (7)$$

where a_{fft} is the maximum free field acceleration in front of the toe; a_{ffc} is the maximum free field acceleration behind the crest and a_{max} is the maximum crest acceleration (Figure 9). The results of numerical analyses are shown in the Table 7.

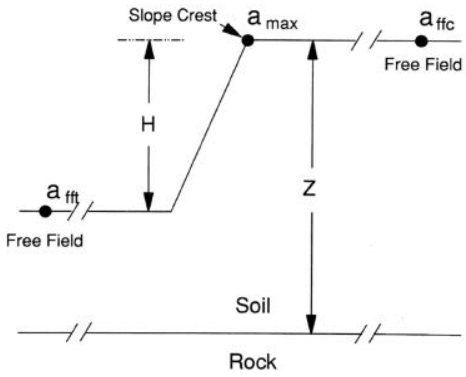

Fig. 9. Ashford et al. [39] model for topographical amplification evaluation

Table 7. Measures of amplifications obtain by numerical analyses

Input	A_t	A_s	A_a
Bottari et al. [29]	0.10	4.29	4.81
Tortorici et al. [30]	0.29	2.76	3.83
Amoruso et al. [31]	0.65	0.76	1.91
DISS Messina Strait	0.22	1.88	2.52
DISS Gioia Tauro	0.01	0.87	0.89
DISS Aspromonte Est	0.09	2.16	2.43
1693 Catania Earthquake	0.16	1.24	1.59

7 Concluding remarks

In this paper, the Performance Based Design (PBD) methodology for the Seismic Microzonation (SM) of ground motion and site effects has been described. The study has been carried out in three main phases: the definition of sets of seven input ground motions for each test site, the definition of the subsoil models and the analysis of the results. The procedure adopted for selecting the suits of waveforms for outcropping and rock conditions has been explained in detail. For the definition of subsoil model in-hole geophysical tests, surface tests and laboratory tests have been carried in order to characterize the soil layers in terms of geometry, geophysical and geotechnical properties. Ground response analyses have been presented by using 1-D and 2-D codes. The main results obtained by numerical analyses have been summarized considering the mean of the values calculated using sets of seven input ground motions. The dynamic response has been investigated in terms of accelerations, response spectra, and amplification functions. Soil amplification factors obtained from site response analyses are high and greater than amplification values provided by Italian technical code [1]. The outcome is presented in terms of preliminary results for the definition of the seismic microzoning map that represents an important tool for the seismic improvement of structures, indispensable for the assessment of seismic hazard.

References

1. NTC D.M. New Technical Standards for Buildings. 2018. Available online: https://www.gazzettaufficiale.it/eli/gu/2018/02/20/42/so/8/sg/pdf
2. Pergalani, F., Pagliaroli, A., Bourdeau, C., et al.: Seismic microzoning map: approaches, results and applications after the 2016–2017 Central Italy seismic sequence. Bulletin of Earthquake Engineering 18:5595–5629 (2020).
3. Pagliaroli, A., Pergalani, F., Ciancimino, A., et al.: Site response analyses for complex geological and morphological conditions: relevant case-histories from 3rd level seismic microzonation in Central Italy. Bulletin of Earthquake Engineering 18:5741–5777
4. Castelli, F., Cavallaro, A., Grasso, S., Lentini, V.: Seismic Microzoning from Synthetic Ground Motion Earthquake Scenarios Parameters: the Case Study of the City of Catania (Italy). Soil Dynamics and Earthquake Engineering, Vol. 88, 2016, 307- 327 (2016)
5. Grasso, S., Maugeri, M.: The Seismic Microzonation of the City of Catania (Italy) for the Maximum Expected Scenario Earthquake of January 11, 1693. Soil Dynamics and Earthquake Engineering, 29 (6): 953-962, (2009). https://doi.org/10.1016/j.soildyn.2008.11.006
6. Grasso, S., Maugeri, M.: The Seismic Microzonation of the City of Catania (Italy) for the Etna Scenario Earthquake (M=6.2) of February 20, 1818. Earthquake Spectra, Vol. 28 (2): 573-594, (2002). https://doi.org/10.1193/1.4000013
7. Grasso, S., Maugeri M.: Seismic Microzonation Studies for the City of Ragusa (Italy). Soil Dynamics and Earthquake Engineering. ISSN: 0267-7261. Vol. 56 (2014): 86–97 (2014)
8. Bonaccorso, R., Grasso, S.; Lo Giudice, E., Maugeri, M.: Cavities and hypogeal structures of the historical part of the City of Catania. Adv. Earthq. Eng., 14, 197–223 (2005)
9. Castelli, F., Grasso, S., Lentini, V., Sammito, M.S.V.: Effects of Soil-Foundation-Interaction on the Seismic Response of a Cooling Tower by 3D-FEM Analysis" Geosciences, 11, 200 (2021) https://doi.org/ 10.3390/geosciences11050200
10. Grasso, S., Massimino, M.R., Sammito, M.S.V.: New Stress Reduction Factor for Evaluating Soil Liquefaction in the Coastal Area of Catania (Italy). Geosciences, 11, 12 (2021) https://doi.org/10.3390/geosciences11010012
11. Maugeri, M., Grasso, S.: Liquefaction potential evaluation at Catania Harbour (Italy). Wit Trans Built Environ., 1, 69–81, (2013) doi:10.2495/ERES130061
12. Castelli, F., Cavallaro, A., Grasso, S.: SDMT soil testing for the local site response analysis. In Proceedings of the 1st IMEKO TC4 International Workshop on Metrology for Geotechnics, Benevento, Italy, 17–18 March 2016; pp. 143–148 (2016)
13. Castelli, F., Grasso, S., Lentini, V., Massimino, M.R.: In situ measurements for evaluating liquefaction potential under cyclic loading. In Proceedings of the 1st 1MEKO TC4 International Workshop on Metrology for Geotechnics, Benevento, Italy, 17–18 March 2016; pp. 79–84 (2016)
14. Boschi, E., Guidoboni, E., Mariotti, D.: Seismic effects of the strongest historical earthquakes in the Syracuse area. Ann. Geofis. 38, 223–253 (1995)
15. Barbano, M.S., Rigano, R.: Earthquake sources and seismic hazard in Southeastern Sicily. Ann. Geofis. 44, 723–738 (2001)
16. Imposa, S., Lombardo, G.: The Etna earthquake of February 20, 1818. In Atlas of Isoseismal Maps of Italian Earthquakes; Postpischl, D., Ed.; Quaderni de La Ricerca Scientifica: Bologna, Italy, 1985; pp. 80–81 (1985)
17. Barbano, M.S., Rigano, R., Cosentino, M., Lombardo, G.: Seismic history and hazard in some localities of south-eastern Sicily. Boll. Geof. Teor. Appl., 42, 107–120 (2001)
18. Castelli, F., Cavallaro, A., Ferraro, A., Grasso, S., Lentini, V., Massimino, M.R.: Dynamic characterisation of a test site in Messina (Italy). Ann Geophys 61(2):222 (2018)

19. Emergeo Working Group: Photographic collection of the coseismic geological effects originated by the 26th December 2018 Etna (Sicily) earthquake. Misc. INGV, 48: 176 (2019)
20. Rovida, A., Locati, M., Camassi, R., Lolli, B., Gasperini, P., Antonucci, A.: Catalogo Parametrico dei Terremoti Italiani (CPTI15), versione 3.0. Istituto Nazionale di Geofisica e Vulcanologia (INGV) (2021) https://doi.org/10.13127/CPTI/CPTI15.3
21. Rovida, A., Locati, M., Camassi, R., Lolli, B., Gasperini P.: The Italian earthquake catalogue CPTI15. Bulletin of Earthquake Engineering, 18(7), 2953-2984 (2020) https://doi.org/10.1007/s10518-020-00818-y
22. Di Maggio, C., Madonia, G., Vattano, M., Agnesi, V., Monteleone, S.: Geomorphological evolution of western Sicily, Italy. Geologica Carpathica 68(1):80–93. (2017) DOI: 10.1515/geoca2017-000
23. Catalano, R., Merlini, S., Sulli, A.,: The structure of western Sicily, Central Mediterranean. Pet. Geosci. 8, 7–18 (2002)
24. Catalano, R., Valenti, V., Albanese, C., Accaino, F., Sulli, A., Tinivella, U., Gasparo Morticelli, M., Zanolla, C., Giustiniani M. 2013: Sicily's fold-thrust belt and slab roll-back: The SI.RI.PRO. seismic crustal transect. J. Geol. Soc., London 170, 3, 451–464 (2013)
25. Cito, P., Iervolino, I.: Peak-over-threshold: quantifying ground motion beyond design. Earthq Eng Struct Dyn. 49(5):458-478 (2020)
26. Iervolino, I., Chioccarelli, E. Convertito, V.: Engineering design earthquakes from multimodal hazard disaggregation. Soil Dynamics and Earthquake Engineering 1212–1231 (2011).
27. Stucchi, M., Meletti, C., Montaldo, V., Crowley, H., Calvi, G. M., Boschi E.: Seismic Hazard Assessment (2003-2009) for the Italian Building Code. Bull. Seismol. Soc. Am. 101(4), 1885-1911 (2011) DOI: 10.1785/0120100130
28. Iervolino, I., Galasso, C., Cosenza, E.: REXEL: computer aided record selection for code-based seismic structural analysis. Bull. Earthquake Eng. 8:339-362 (2010) DOI 10.1007/s10518-009-9146-1
29. Bottari, A., Carapezza, E., Carapezza, M., Carveni, P., Cefali, F., Lo Giudice, E., Pandolfo, C.: The 1908 Messina strait earthquake in the regional geostructural framework. J. Geodyn. 5, 275–302. (1986)
30. Tortorici, L., Monaco, C., Tansi, C., Cocina, O.: Recent and active tectonics in the Calabrian Arc (Southern Italy). Tectonophysics, 243, 37–55 (1995)
31. Amoruso, A., Crescentini, L., Scarpa, R.: Source parameters of the 1908 Messina Strait, Italy, earthquake from geodetic and seismic data. J. Geophys. Res. 107, ESE 4-1–ESE 4-11 (2002)
32. Valensise, G., Pantosti, D.: Database of potential sources for earthquakes larger than M 5.5 in Italy. Ann. Geophys. 44, 1–964 (2001)
33. Castelli, F., Cavallaro, A., Grasso, S.; Ferraro, A. In situ and laboratory tests for site response analysis in the ancient city of Noto (Italy). Proceedings of the 1st IMEKO TC4 International Workshop on Metrology for Geotechnics, Benevento, Italy, 17–18 March 2016; pp. 85–90 (2016)
34. Kottke, A.R., Rathje, E.M.: Technical Manual for STRATA. PEER Report 2008/10; Univ. of California: Berkeley, CA, USA (2008)
35. Ferraro, A., Grasso, S., Massimino, M.R.: Site effects evaluation in Catania (Italy) by means of 1-D numerical analysis. Ann. Geophys., 61 (2018)
36. Yokota, K., Imai, T., Konno, M.: Dynamic Deformation Characteristics of Soils Determined by Laboratory Tests. OYO Tec. Rep. 3, 13-37 (1981)
37. Krahn, J.: Dynamic Modeling with QUAKE/W: An Engineering Methodology; GEO-SLOPE International Ltd.: Calgary, AB, Canada, (2004)
38. Dipartimento della Protezione Civile e Conferenza delle Regioni e delle Province Autonome: Indirizzi e criteri per la microzonazione sismica, available at https://www.protezionecivile.gov.it
39. Ashford, S.A., Sitar, N., Asce, M.: Simplified method for evaluating seismic stability of steep slopes. J. Geotech. Geo-Environ. Eng. 128, 119–128 (2002)